

Dense gas properties in a strongly-lensed wet merger: bridging the gap between local ULIRGs and high- z systems

PI: T. K. Daisy Leung

Missing link between mergers/ULIRGs and their high- z analogues Ultraluminous infrared galaxies (ULIRGs: $L_{\text{IR}} \geq 10^{12} L_{\odot}$) have been regarded as analogues of high-redshift (z) starbursts given the similarities in their interstellar medium (ISM; e.g. $L_{\text{IR}}/L'_{\text{CO}}$). As such, detailed studies of ULIRGs are important to gain more detailed insight into the early universe and in studies of galaxy evolution over cosmic time. While mergers are believed to play an important role in giving rise to these dusty galaxies (e.g. Sanders & Mirabel 1996), merger-induced effects on the physical mechanisms and chemistry that drive the starburst (SB) and active galactic nucleus (AGN) activities on small scales are still unclear.

While the ISM in local ULIRGs has been studied in great detail, forming a rich inventory of molecular transitions that serves as the template for studying high- z galaxies (e.g., Rangwala et al. 2015), a wide knowledge gap persists between $z=0$ and the epoch when most stars are formed in the universe ($z \sim 2$). Here we aim to bridge this gap by testing local correlations and properties at high redshifts by observing the dynamical structure and properties of the ISM of the quadruply lensed galaxy RXJ1131-1231 (henceforth RX1131) and its dust-obscured companion at $z_{\text{CO}} \sim 0.65$ (Fig. 1).

Molecular gas in AGN/SB Extreme star formation rates (SFRs) in ULIRGs and their high- z analogues are a natural consequence of either gas being converted into stars more efficiently and/or their high molecular gas fractions, which would lead to fragmentation of giant star-forming clumps and turbulent conditions due to gravitational instability. Indeed, observations at $z=1-2$ have found gas clumps of size \sim few kpc (Swinbank et al. 2012a,b), which are much bigger than those in normal star-forming galaxies. Therefore, resolving the gas dynamics on sub-kpc scales is important to understand the mechanisms and physical processes responsible for the different star-formation modes in normal galaxies and ULIRGs.

While ^{12}CO emission traces the total molecular distribution and dynamics, high-dipole moment molecules such as HCN and HCO^+ are expected to trace the denser, actively star-forming gas. Indeed, a tight correlation between $\text{HCN}(J=1 \rightarrow 0)$ and L_{IR} (a proxy for SFR) has been found in nearby galaxies and local giant molecular clouds (GMCs; Gao & Solomon 2004, hereafter GS04; Wu et al. 2005), suggesting HCN is a faithful tracer of the star-forming dense gas. However, higher- J transitions (e.g. $J=4 \rightarrow 3$) have also been suggested to be better proxies of the star-forming gas since they trace the much denser gas ($n \gtrsim 10^5 - 10^7 \text{ cm}^{-3}$) that is thought to be the immediate fuel for SF in turbulent GMCs (Shirley et al. 2003; Krumholz & McKee 2005). This is supported by the linear correlations found in $L_{\text{IR}} - L'_{\text{HCN}(J=4 \rightarrow 3)}$ and $L_{\text{IR}} - L'_{\text{HCO}^+(J=4 \rightarrow 3)}$ (Zhang et al. 2014). Since the ground state lines are redshifted to frequencies beyond the spectral coverage of ALMA at $z > 0.06$, it is important to establish diagnostics using these mid- J lines to study distant galaxies. Due to the difference in abundances and excitation conditions of HCN and HCO^+ in star-forming versus AGN regions, the line ratio $\text{HCN}(J=4 \rightarrow 3)/\text{HCO}^+(J=4 \rightarrow 3)$ has been proposed as a diagnostic tool to reveal deeply-buried AGNs at the cores of ULIRGs (Imanishi & Nakanishi 2014; García-Burillo et al. 2014; Viti et al. 2014; Izumi et al. 2016; Imanishi et al. 2016).

Prior to ALMA, studies using dense gas tracers were largely limited to the local universe ($z \lesssim 0.1$) with only five detections at $z \gtrsim 0.3$ (e.g., Riechers et al. 2007, 2010; Wagg et al. 2005; Gao et al. 2007). Moreover, none of these spatially resolve the emission, rendering it difficult to draw more detailed conclusions on the dense gas properties of galaxies at high z . Even with ALMA, such studies will remain challenging, but by combining the magnification provided by gravitational lensing with the exceptional spatial resolution and sensitivity of ALMA, studies of dense molecular gas in distant galaxies are now possible, as proposed here.

Science Target RXJ 1131-1231: a demonstrative case at $z \sim 0.7$

RX1131 is a quadruply imaged AGN with its host galaxy lensed into a partial Einstein ring (Fig. 1). HST observations (rest-frame UV) have revealed distinct emission from recent star-formation (lensing arcs) and from the AGN (bright knots) in the background galaxy (Sluse et al. 2003), demonstrating the great potential for probing its ISM conditions in detail. Lens modeling carried out on optical images shows that the AGN

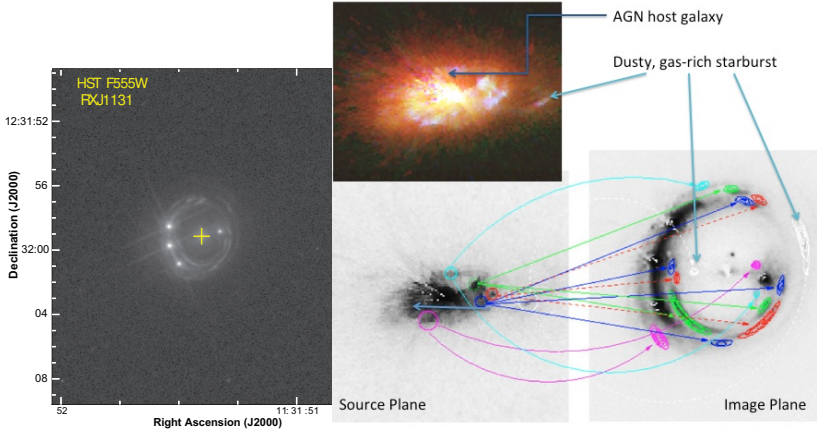


Figure 1: **Stellar light distribution in the AGN host galaxy of RXJ 1131-1231 and its reconstructed source plane morphology.** *Left:* The rest-frame UV emission (tracing recent star-formation) is lensed into an almost complete Einstein ring with diameter $\sim 3.8''$. *Right:* Lens modeling of the optical emission identifies complex structures in the host galaxy and an optically faint companion (white component as indicated by the blue arrows; Claeskens et al. 2006), which we have recently confirmed by lens-modeling CO($J=2 \rightarrow 1$) emission detected with NOEMA (Fig. 4; Leung & Riechers, in prep.). Here we propose to study the ISM conditions in this AGN-starburst merger with finer detail than otherwise possible with current facilities.

resides in a star-forming region of size ~ 1 kpc in its host galaxy, which itself is 7 kpc across, and made it possible to identify seven distinct structures in the source plane (Fig. 1). A companion galaxy of size ~ 700 pc across was also identified at ~ 2.4 kpc away from the AGN host galaxy in the HST observations (Brewer & Lewis 2008). We recently confirmed that both galaxies are at the same redshift by detecting their CO($J=2 \rightarrow 1$) emission and lens-modeling their gas distribution in velocity space (Fig. 4f), verifying that both are gas-rich (Leung & Riechers, in prep.). Our SED modeling of the dust continuum emission up to $250 \mu\text{m}$ finds $L_{\text{IR}} \sim 6 \times 10^{12} L_{\odot}$ (corrected for lensing). Hence, this target is a gas-rich ULIRG merger at $z \sim 0.7$ caught in the act.

Proposed Observations and Science Goals Here we propose to map (1): CO($J=5 \rightarrow 4$) at $0.15''$ resolution (~ 500 pc at $z \sim 0.7$ in the source plane) and (2): HCN($J=4 \rightarrow 3$) and HCO $^{+}$ ($J=4 \rightarrow 3$) emission and the underlying continuum at $0.7''$ resolution (2.5 kpc in the source plane). The continuum will provide an additional constraint on the Rayleigh-Jeans tail of the dust emission, which is currently constrained by four photometric data. This will reduce the uncertainties on the the gas-to-dust ratio, dust temperature(s), dust mass, and its spatial extent (and thus the surface density of the SFR). These quantities are important for investigating how the ISM varies as galaxies evolve across cosmic time. In conjunction with the large set of ancillary data (from rest-frame UV to radio wavelengths, including our recent observations of CO($J=2 \rightarrow 1$) and CO $J=3 \rightarrow 2$), our proposed observations are designed to investigate:

(1) Dynamics and kinematics Our CO($J=2 \rightarrow 1$) data obtained with NOEMA shows an asymmetric double-horned line profile (Fig. 4a). Given the 1st moment map and the observed velocity gradient across the source plane in our model (Fig. 4d, f), this is indicative of a kinematically ordered galaxy, but its emission has been lensed differentially. Limited by the spatial resolution of this data, it is not possible to infer the true kinematics due to beam smearing. Furthermore, the unusually high velocity dispersion ($\gtrsim 400 \text{ km s}^{-1}$) in the central region (Fig. 4e) hints at perturbations from the AGN, internal turbulence due to interactions with the companion, and/or instability due to the huge gas reservoir. Therefore, higher-resolution CO($J=5 \rightarrow 4$) imaging, as proposed here, is needed to distinguish between a merger-driven and a turbulent clumpy disk starburst.

The requested resolution for CO($J=5 \rightarrow 4$) is critical as it allows us to obtain a detailed dynamical lens model of the system and therefore probe structure at sub-kpc scales (typical size of high- z GMCs), as well as enables us to compare the spatial distributions of star-forming gas clumps with recent star-formation (from HST). Such comparisons are the key for understanding different processes that regulate the SB in ULIRGs/mergers and examining how they differ from other galaxy populations. We will also measure the linewidths of the very dense gas (traced by HCN and HCO $^{+}$), the highly excited warm gas (traced by CO $J=5 \rightarrow 4$), and the more-extended, less-perturbed molecular gas (traced by low- J CO) at various regions within the AGN host galaxy to constrain the kinematics and relative mass-fractions of different gas phases, which are indicative of the evolutionary stage of this galaxy.

(2) Line ratios and the AGN/SB diagnostic Aided by lensing, we will be able obtain kinematical information on spatial scales smaller than the beam, as seen in our CO($J=2\rightarrow1$) data (Fig. 4c, d), thereby enabling us to probe the physical properties of the inner molecular disk near the AGN of RX1131. Recent studies find that the HCN($J=4\rightarrow3$)/HCO⁺($J=4\rightarrow3$) line ratio is enhanced in the circumnuclear disk (CND) near AGNs, and falls off with distance from the CND (García-Burillo et al. 2014; Imanishi et al. 2016). At the proposed resolution, we will resolve the line emission originating near the AGN and that from the spatially extended SB regions ($>kpc$ scales) in the host galaxy. By measuring spatial variations in this line ratio, we will assess its utility as an AGN/SB diagnostic (Fig. 2) at $z\sim0.7$. Since the HCN vibrational line ($v_2=1; J=4\rightarrow3$) falls within the targeted frequency range, we will use it to independently constrain the radiation properties of the AGN environment, given that this line is excited by infrared pumping of the same radiation field associated with the AGN that causes the elevated HCN($J=4\rightarrow3$)/HCO⁺($J=4\rightarrow3$) (Sakamoto et al. 2010; Imanishi & Nakanishi 2013). The proposed spatial resolution is also necessary for a detailed lens modeling of each emission line, enabling measurements of reliable line ratios without significant uncertainties due to differential lensing.

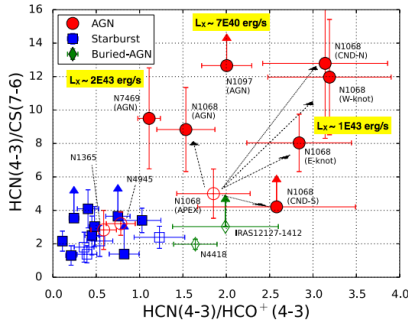


Figure 2: HCN($J=4\rightarrow3$)/HCO⁺($J=4\rightarrow3$) as AGN/SB diagnostic. Differences in line ratios between local AGNs, SBs, and (U)LIRGs with buried AGNs suggest that HCN($J=4\rightarrow3$)/HCO⁺($J=4\rightarrow3$) can be used as a diagnostic tool to distinguish between the energy source from an AGN and starburst, where an elevated line ratio is seen in AGN-dominated regions relative to starbursts. Such diagnostics depend heavily on the spatial resolution, as demonstrated by the measurements taken with APEX (empty circle) and ALMA (filled circles) in NGC1068. We here propose to spatially resolve this line ratio within RX1131 in order to assess its utility as an AGN/SB diagnostic at high redshift. (Figure taken from Izumi et al. 2016)

In addition, we will use spatially resolved line ratios of HCN/CO and HCO⁺/CO within RX1131 as proxies of its very dense (cores; $\sim 10^5\text{-}10^7\text{ cm}^{-3}$) versus the less dense (clumps; $\sim 10^4\text{ cm}^{-3}$) gas content and their spatial distributions as a function of distance from the AGN. This will enable us to use relations such as HCN/CO- L_{IR} to investigate the main driver of the enhanced SFRs in ULIRGs (e.g., if the dense gas distribution and content toward the central region of RX1131 is consistent with other ULIRGs). Measuring the gas kinematics and variations in these line ratios will thus provide clues on how galaxy interactions drive gas into inner disks to initiate SB/AGN activity and how the excitation of gas differs from normal star-forming galaxies. We will also combine CO($J=5\rightarrow4$) with our existing CO($J=2\rightarrow1$) and CO($J=3\rightarrow2$) data to constrain the gas density (n_{H_2}) and kinetic temperature by performing large velocity gradient (LVG) modeling.

(3) The SK Law for dense gas The Schmidt-Kennicutt (SK) relation ($\Sigma_{\text{SFR}} \propto \Sigma_{\text{gas}}^N$; Fig. 3) is one of the key ingredients for theoretical models of galaxy evolution since it encodes the physical processes and timescales regulating star-formation and their dependence on the ISM (e.g., Narayanan & Krumholz 2014). However, the surface density of gas at high densities ($n \gtrsim 10^5\text{ cm}^{-3}$; Σ_{dense}) is poorly constrained for high- z galaxies due to the lack of *spatially resolved* observations of the much weaker emission from high critical density tracers. It is therefore unclear how the power-law index of the SK relation should change depending on the critical density of the tracer used to probe the SF gas (e.g., Krumholz & Thompson 2007) and how the SFR surface density could differ between normal galaxies and mergers depending on their global dynamical timescales. At the proposed resolution, we will spatially resolve, for the first time, the *true SK relation* by measuring the *dense* gas surface density in a high- z merger, down to the size scale of star-forming gas clumps. This will provide crucial constraints on the conditions for star-formation at high redshift.

In summary, our proposed observations provide an exceptional opportunity to investigate the physical properties and dynamical structures of different gas phases in the ISM of a distant merger at exquisite detail. Our proposed observations of the HCN and HCO⁺ lines will also demonstrate the capabilities of ALMA to utilize these much fainter high-dipole moment molecules as routine tracers to study star-formation at earlier cosmic epochs.

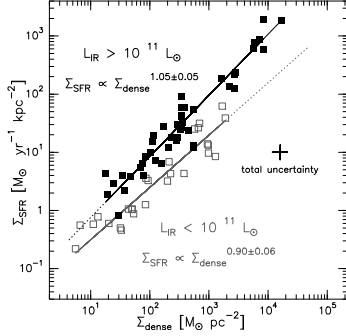


Figure 3: Schmidt-Kennicutt relation for dense gas. While constraints on the power-law index from gas of different densities are important for star-formation models, current studies only have constraints on gas of densities below n_{crit} of the ground state transition of HCN ($n_{\text{crit}} \sim 10^4$). These studies are also largely limited to measurements of local galaxies (García-Burillo et al. 2012). Our proposed observations will, for the first time, constrain the spatially resolved SK relation at kpc scales in a ULIRG at $z \sim 0.7$ using high critical density tracers (HCN $J=4 \rightarrow 3$ and $\text{HCO}^+ J=4 \rightarrow 3$). This will allow us to explore potential deviations at higher redshift and provide key constraints for models of galaxy evolution.

Technical overview We estimate the source size from our lens model and adopt line ratios measured for ULIRGs and high- z starbursts (GS04; P07; Greve et al. 2009; Carilli & Walter 2013) to compute the expected line fluxes. To secure enough S/N for lens modeling, we require a minimum of 8σ of $\sigma = 0.47 \text{ mJy beam}^{-1}$ and $\sigma = 0.07 \text{ mJy beam}^{-1}$ per 150 km s^{-1} channel for the science goals, respectively (see TJ for details).

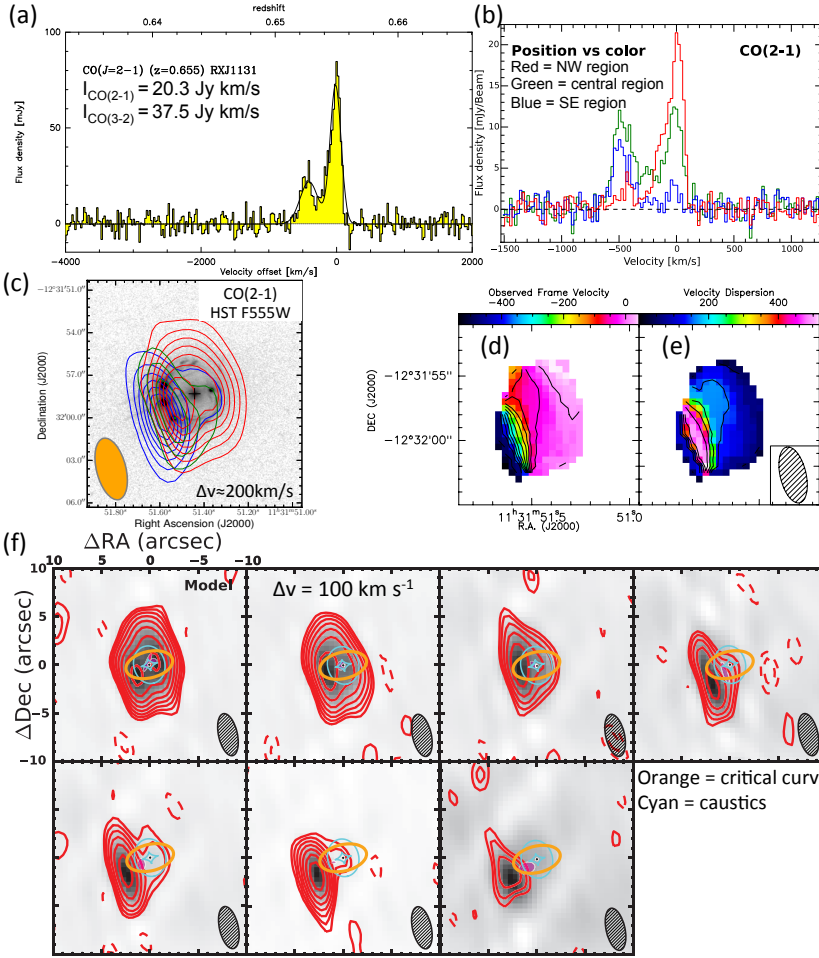


Figure 4: Recent CO($J=2 \rightarrow 1$) data from NOEMA. (a): A double-horned line profile from the AGN host galaxy, which appears asymmetric due to differential lensing. (b): Spectra taken at three locations along the strongest velocity gradient, demonstrating differential lensing of the kinematic components of the gas-rich “disk”. (c): Observed spatial variations across different velocity components due to differential lensing, as shown by the red (red-shifted), green (line center), and blue (blue-shifted) contours. (d, e): The observed velocity gradient and velocity dispersion are suggestive of a kinematically ordered disk at the current resolution limit. The spectrally resolved lensed emission allows us to probe dynamical structures on smaller spatial scales than otherwise possible. (f): Channel maps of the CO emission (red) overlaid on our best-fit lens models (grayscale). The foreground lensing galaxy is represented by a black dot. The reconstructed source morphology (magenta ellipses) is also suggestive of a “disk”. Given the presence of a companion galaxy within 2.4 kpc and beam smearing effects, high-resolution imaging is necessary to unambiguously determine the structure that gives rise to the observed velocity gradient and dispersion, as proposed here. This will allow us to investigate the mechanisms responsible for driving the starburst in RX1131 and its ISM conditions as it interacts with the companion. We therefore aim to spatially resolve the gas dynamics, kinematics and ISM conditions in a wet-merger, providing observational constraints on the star-formation processes at an epoch where the SFR density is steeply rising across cosmic times.

References • Brewer et al. 2008, MNRAS, 390, 39 • Carilli et al. 2013, ARA&A, 51, 105 • Claeskens et al. 2006, A&A, 451, 865 • Gao et al. 2007, ApJ, 660, L93 • Gao et al. 2004, ApJ, 606, 271 • García-Burillo et al. 2014, A&A, 567, A125 • García-Burillo et al. 2012, A&A, 539, A8 • Greve et al. 2009, ApJ, 692, 1432 • Imanishi et al. 2013, AJ, 146, 91 • Imanishi et al. 2014, AJ, 148, 9 • Imanishi et al. 2016, ArXiv e-prints • Izumi et al. 2016, ApJ, 818, 42 • Juneau et al. 2009, ApJ, 707, 1217 • Krumholz et al. 2005, ApJ, 630, 250 • Krumholz et al. 2007, ApJ, 669, 289 • Narayanan et al. 2014, MNRAS, 442, 1411 • Papadopoulos, P. P. 2007, ApJ, 656, 792 • Rangwala et al. 2015, ApJ, 806, 17 • Riechers et al. 2007, ApJ, 671, L13 • Riechers et al. 2010, ApJ, 725, 1032 • Sakamoto et al. 2010, ApJ, 725, L228 • Shirley et al. 2003, ApJS, 149, 375 • Sluse et al. 2003, A&A, 406, L43 • Swinbank et al. 2012a, ApJ, 760, 130 • Swinbank et al. 2012b, MNRAS, 426, 935 • Viti et al. 2014, A&A, 570, A28 • Wagg et al. 2005, ApJ, 634, L13 • Wu et al. 2005, ApJ, 635, L173 • Zhang et al. 2014, ApJ, 784, L31